Hyperglycemia Induces a Dynamic Cooperativity of Histone Methylase and Demethylase Enzymes Associated With Gene-Activating Epigenetic Marks That Coexist on the Lysine Tail

Daniella Brasacchio,[1] Jun Okabe,[1] Christos Tikellis,[2] Aneta Balcerczyk,[1] Prince George,[1] Emma K. Baker,[1] Anna C. Calkin,[2] Michael Brownlee,[3] Mark E. Cooper,[2,3] and Assam El-Osta[1]

OBJECTIVE—Results from the Diabetes Control Complications Trial (DCCT) and the subsequent Epidemiology of Diabetes Interventions and Complications (EDIC) Study and more recently from the U.K. Prospective Diabetes Study (UKPDS) have revealed that the deleterious end-organ effects that occurred in both conventional and more aggressively treated subjects continued to operate >5 years after the patients had returned to usual glycemic control and is interpreted as a legacy of past glycemia known as "hyperglycemic memory." We have hypothesized that transient hyperglycemia mediates persistent gene-activating events attributed to changes in epigenetic information.

RESEARCH DESIGN AND METHODS—Models of transient hyperglycemia were used to link NFκB-p65 gene expression with H3K4 and H3K9 modifications mediated by the histone methyltransferases (Set7 and SuV39h1) and the lysine-specific demethylase (LSD1) by the immunopurification of soluble NFκB-p65 chromatin.

RESULTS—The sustained upregulation of the NFκB-p65 gene as a result of ambient or prior hyperglycemia was associated with increased H3K4m1 but not H3K4m2 or H3K4m3. Furthermore, glucose was shown to have other epigenetic effects, including the suppression of H3K9m2 and H3K9m3 methylation on the p65 promoter. Finally, there was increased recruitment of the recently identified histone demethylase LSD1 to the p65 promoter as a result of prior hyperglycemia.

CONCLUSIONS—These studies indicate that the active transcriptional state of the NFκB-p65 gene is linked with persisting epigenetic marks such as enhanced H3K4 and reduced H3K9 methylation, which appear to occur as a result of effects of the methyl-writing and methyl-erasing histone enzymes. *Diabetes* **58:1229–1236, 2009**

Vascular complications are the major source of morbidity and mortality in diabetes and are considered, based on both epidemiological data and from more mechanistic studies, to occur primarily as a result of the long-term deleterious effects of hyperglycemia. Interestingly, these vascular complications often persist and may progress despite improved glucose control, possibly as a result of prior episodes of hyperglycemia. Results in both type 1 and type 2 diabetes, as observed in the Diabetes Control and Complications Trial (DCCT)/Epidemiology of Diabetes Interventions and Complications (EDIC) Study and in the recent follow-up of the U.K. Prospective Diabetes Study (UKPDS), have revealed that end-organ effects that occurred in both conventional and intensified glycemic control groups continued to operate >5 years after the patients had returned to their usual level of glycemic control (1,2). These studies suggest that the injurious effects of exposure to high glucose levels persist for many years after these episodes of altered metabolic control and this is typically referred to as either "hyperglycemic memory" (3) or the legacy effect (4). Recently, several clinical trials, including the ADVANCE (5) and ACCORD studies (6), failed to demonstrate that intensified glycemic control for 3–5 years markedly reduced macrovascular complications, emphasizing the lack of rapid reversibility of glucose-related vascular changes by improved glycemic control. Indeed, such studies are consistent with the view that previous episodes of transient hyperglycemia may induce longstanding deleterious changes in the vasculature.

Until now, our view of the susceptibility to hyperglycemia-induced vascular complications focused predominantly on genetic polymorphisms, but recent studies exploring epigenetic mechanisms such as chromatin remodeling, histone modifications, and DNA methylation are increasingly appreciated to be critical to the way we view changes in gene activity. This gene-environment interaction involving epigenetic changes may be particularly relevant to the pathogenesis of diabetes complications (7) and conferring epigenetic marks by specifically modulating histone methylation (8). In this study, we have extended these findings to characterize in more detail the nature of histone methylation of the promoter region of the NFκB-p65 gene, which is upregulated in a sustained manner in response to prior transient hyperglycemia (3). These results highlight the importance of histone modifications that control gene activity, which is linked with

persisting epigenetic marks that are specifically maintained when the endothelial cell is out of its previous hyperglycemic milieu.

RESEARCH DESIGN AND METHODS

In vitro studies

Cell culture conditions and treatments. Confluent bovine aortic endothelial cells were maintained in minimum essential medium (Gibco) containing 0.5% fetal bovine serum, nonessential amino acids (Gibco), and antibiotics Gentamicin (Pfizer). Cells were incubated with minimum essential medium with 5.5 mmol/l low glucose or minimum essential medium with 30 mmol/l high glucose or 30 mmol/l mannitol for 16 h where stated.

Set7 shRNA knockdown. Human microvascular endothelial cells (HMECs) were infected with MISSION shRNA-expressing lentiviral vectors targeted to Set7 coding regions according to the user instructions (Sigma). The sequence targeting Set7 corresponds to 5′-CCAGATCCTTATGAATCA-GAA-3′ (TRCN0000078630). Cells transduced with MISSION Non-Target shRNA Control Vector were used as controls. HMECs were seeded at 5×10^5 cells/dish in a 60-mm dish 20 h before infection, incubated with the lentivirus for 2 days, followed by selection in puromycin (1 µg/ml; Sigma) for 7 days. The cells were examined by protein blots using anti-Set7 rabbit antibody.

Overexpression of Set7 in human endothelial cells. HMECs expressing Set7 were created by retrovirus-mediated gene transfer as described previously (9). cDNAs encoding FLAG-tagged Set7 were inserted between the *Bam*HI and *Not*I sites of the retroviral vector pCX4neo (10) (a gift from Dr. T. Akagi, KAN Research Institute, Kobe, Japan) to create pJS14. pJS14 or pCX4neo was co-transfected with retrovirus packaging vectors (Takara) into 293T cells (10). Two days after transfection, culture supernatants were collected and used as viral stocks. HMECs were seeded at 5×10^5 cells/dish in a 60-mm dish 20 h before infection, incubated with the virus stock for 2 days, followed by selection in Geneticin (G418, 1 mg/ml; Invitrogen) for 7 days. The cells were then examined by protein blots using anti-FLAG M2 monoclonal antibody (Sigma) and anti-Set7 rabbit serum (a gift from Dr. P.L. Jones, University of Illinois) (7).

Immunoprecipitation of FLAG-Set7. Cell lysates were prepared from cells expressing FLAG-Set7 or from cells transduced with pCX4neo as a control. The 1×10^7 cells were washed twice with ice-cold PBS and extracted with 600 µl lysis buffer (50 mmol/l Tris HCl, pH 7.5, 150 mmol/l NaCl, 1 mmol/l EDTA, 1% Triton X-100, and proteinase inhibitor). Lysate was incubated with anti-FLAG M2 affinity gel (Sigma) for 2 h at 4°C. Immunoprecipitates were washed with Tris-buffered saline (50 mmol/l Tris HCl, pH 7.5, 150 mmol/l NaCl) three times and then eluted with $3\times$ FLAG peptide (Sigma) and analyzed by immunoblotting as well as measuring histone methyltransferase activity.

Histone methyltransferase activity assay. The histone methyltransferase activity assay was performed according to the manufacturer's (Upstate) instructions. One of the following substrates was used for methyltransferase reactions: 5 µg recombinant histone H3 (Upstate) or 0.4 nmol of a biotin-conjugated histone H3 peptide (amino acids 1–23), either K4 or R4 (Sigma). Reactions were determined by spotting on P-81 paper (Upstate) and scintillation counting.

Chromatin immunoprecipitation. Cells were treated with formaldehyde at a 1% concentration for 10 min and then treated with glycine at 0.15 mol/l for 10 min. Cell pellets were resuspended in SDS lysis containing 1% SDS, 10 mmol/l EDTA, 50 mmol/l Tris, pH 8.1 (Upstate), and a protease inhibitor cocktail (Roche). Cells were sonicated to shear chromatin to 700–300 bp in length, resuspended in chromatin immunoprecipitation dilution buffer containing 0.01% SDS, 1.1% Triton X-100, 1.2 mmol/l EDTA, 16.7 mmol/l Tris-HCl, pH 8.1, and 167 mmol/l NaCl, and 15 µl salmon sperm DNA-protein A agarose (Upstate) was added and precleared. To the soluble chromatin fraction, the following antibody of interest was added and incubated for a minimum of 8 h: H3K4m1 (Abcam ab8895), H3K4m2 (Upstate 07030), H3K4m3 (Upstate 07473), H3K9m1 (Abcam ab9045), H3K9m2 (Abcam ab7312–100), H3K9m3 (Abcam ab8898), Set7 (a gift from Dr. P Jones, University of Illinois at Urbana-Champaign), LSD1 (Upstate 05939), and Suv39h1 clone MG44 (Upstate 05615). Immune complexes were collected with salmon sperm DNA-protein A agarose and subsequently washed and eluted with buffer (1% SDS, 0.1 mol/l NaHCO$_3$). Protein-DNA cross-links were reversed overnight at 65°C and recovered by phenol-chloroform extraction and ethanol precipitated at −20°C. Analysis of chromatin immunoprecipitation DNA samples was performed by quantitative PCR (qPCR) of the nuclear factor (NF)-κB p65 promoter region (sequences available on request). An input sample was used as an internal control for variation in DNA between samples.

RNA isolation and first-strand cDNA synthesis. Total RNA was extracted using Trizol preparation. Cells were subsequently treated with Turbo DNAse (Ambion). First-strand cDNA synthesis from the purified mRNA was performed using M-MLV Reverse Transcriptase (Invitrogen) according to the manufacturer's instructions. The NFκB p65 gene was quantified using qRT-PCR.

RT-PCR. PCR amplification was performed using ABI Prism 7500; 2 pmol of each forward and reverse primer was added to a total of 20 µl reaction containing 1× SYBR Green qPCR SuperMix-UDG and Rox Reference Dye (Invitrogen). Reactions were incubated for 50°C for 2 min and 95°C for 10 min, followed by 50 cycles of 95°C for 15 s and 60°C for 1 min.

In vivo studies

Animal model. Male apolipoprotein knockout (apoE KO) mice (backcrossed 20 times to a C57BL/6 background; Animal Resource Centre, Canning Vale, WA, Australia) were housed at the Precinct Animal Centre, Baker IDI Heart and Diabetes Institute, and studied according to guidelines of the National Health and Medical Research Council of Australia. At week 7, mice were rendered diabetic via five daily intraperitoneal injections of 55 mg · kg^{-1} · day^{-1} streptozotocin (MP Biomedicals, Eschwege, Germany), resulting in a model of insulin deficiency (11). ApoE and apoE diabetic mice were monitored for 20 weeks. In over 90% of mice injected with these five daily injections of streptozotocin, plasma glucose levels were >20 mmol/l within the first week of the study. In all injected mice, plasma glucose levels were measured every 2 weeks. This serial monitoring revealed that in a subgroup of mice (<20%), despite initially developing hyperglycemia, after ~10–12 weeks, these mice now had reduced plasma glucose levels (<15 mmol/l) despite no treatment, which remained decreased until the time of death at week 20. This group was termed "previously hyperglycemic" (HG→NG) and was compared to the control (NG→NG) and diabetic (HG→HG) mice. All these apoE KO mice received standard mouse food and water ad libitum. Mice were culled by euthanasia using an intraperitoneal injection of Euthal (10 mg/kg) (Delvet Limited, Seven Hills, Australia) followed by exsanguination via cardiac puncture. The excised aortas were placed in 10% neutral buffered formalin and quantitated for lesion area before being processed for subsequent immuno-histochemical analysis. In a subset of animals, aortas were snap-frozen in liquid nitrogen and stored at −70°C for subsequent RNA extraction.

Metabolic parameters. Erythrocytes were collected at death for measurement of glycated hemoglobin by high-performance liquid chromatography. Plasma glucose levels were measured using an automated system (Abbott Architect ci8200, Abbott Laboratories). At death, plasma lipids were measured by an autoanalyzer (11).

Isolation of total RNA, synthesis of cDNA, and quantitative real-time PCR. Gene expression of NFκB p65, vascular adhesion molecule 1 (VCAM-1), and macrophage chemoattractant protein 1 (MCP-1) were assessed by real-time qPCR. This was performed using the TaqMan system based on real-time detection of accumulated fluorescence (ABI Prism 7500; Perkin-Elmer, PE Applied Biosystems, Foster City, CA), as previously used by our group (12). Briefly, whole aorta was homogenized using the Ultra-Turrax (Janke & Kunkel IKA, Labortechnik, Germany) in TRIZOL (Life Technologies, Gaithersburg, MD), and total RNA was isolated. cDNA was synthesized with a reverse transcriptase reaction using the Superscript First Strand Synthesis System for RT-PCR (Life Technologies) with random hexamers, dNTPs, and total RNA extracted from mouse aortas. To assess genomic DNA contamination, controls without reverse transcriptase were included. Briefly, gene-specific 5′-oligonucleotide primer, 3′-oligonucleotide primer, and MGB FAM-probe corresponding to each gene (sequences available upon request) were designed using the software program Primer Express (PE Applied Biosystems). The generation of amplicons was defined as the point during cycling when amplification of the PCR product is first detected above the threshold setting.

The RT-PCR took place with 500 nmol/l of forward and reverse primer and 50 nmol/l of FAM/MGB probe and VIC 18S ribosomal probe, in 1× Taqman universal PCR master mix (PE Biosystems). Each sample was run and analyzed in triplicate. Gene expression was normalized to 18S mRNA with samples from the control (NG→NG) aorta used as the calibrator with a given value of 1, and all other groups were compared with this calibrator group.

Plaque area quantitation. Plaque area was quantitated as described previously (11). In brief, aortas removed from the mice were cleaned of excess fat under a dissecting microscope and subsequently stained with Sudan IV-Herxheimer's solution (0.5% wt/vol) (Gurr, BDH Limited). Aortas were dissected longitudinally; divided into arch, thoracic, and abdominal segments; and pinned flat onto wax. Images were acquired with a dissecting microscope equipped with an Axiocam camera (Zeiss, Heidelberg, Germany). Total and segmental (i.e., arch, thoracic, and abdominal) plaque area was quantitated as the percentage area of aorta stained red (Adobe Photoshop v7.0).

Statistical analysis. Data are shown as means ± SE. One-way nonparametric ANOVA for repeated measures followed by Fisher's post hoc test was used to compare treatment groups. Calculations were performed using GraphPad Prism (Graphpad Software).
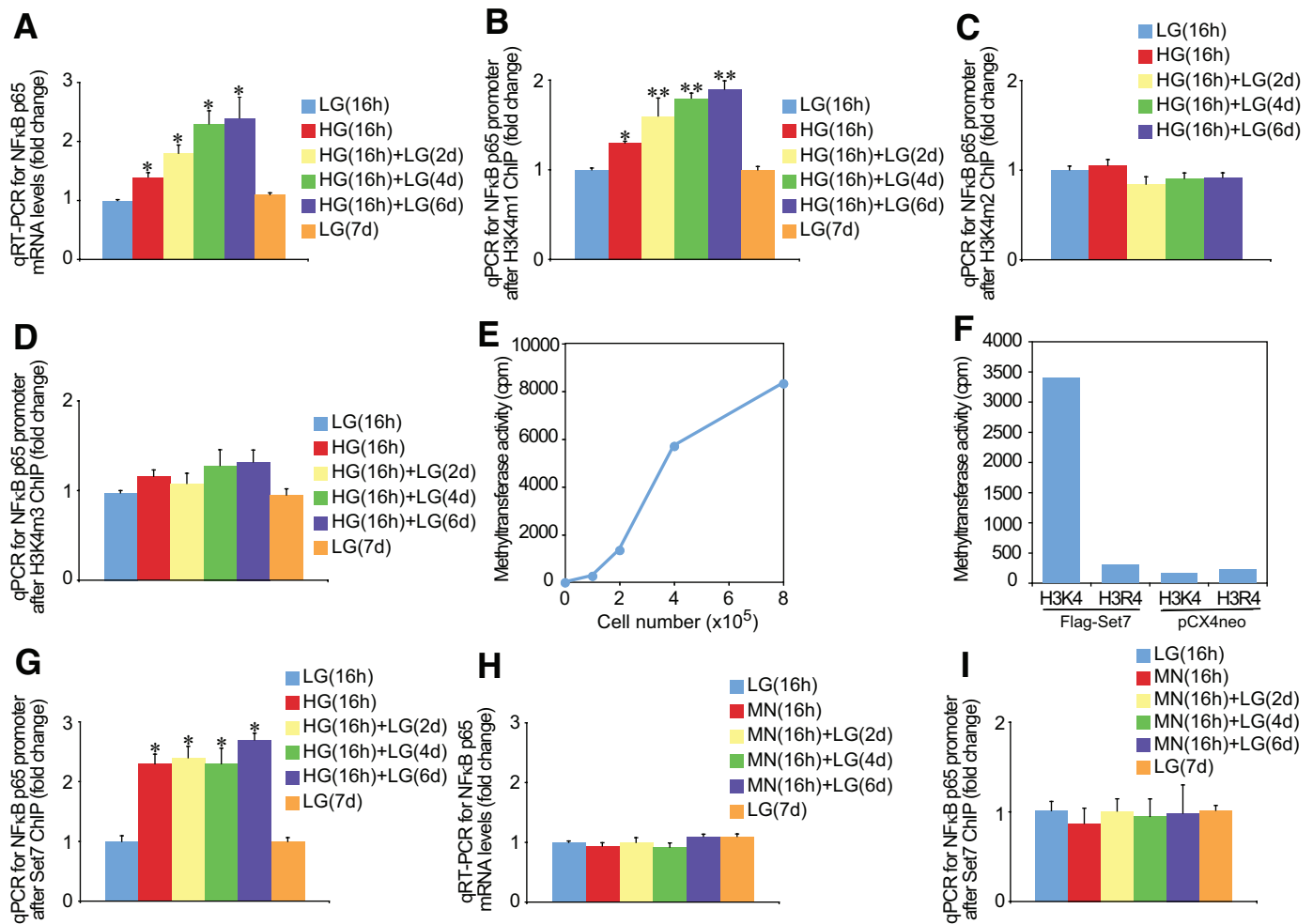
FIG. 1. Ambient and prior hyperglycemia sustains increased activating H3K4m1-associated Set7 enrichment on the NFkB-p65 gene in aortic endothelial cells. *A*: Ambient and prior hyperglycemia sustains increased NFkB-p65 gene expression in bovine aortic endothelial cells. RNA was extracted, and NFκB-p65 mRNA levels were quantified by real-time RT-PCR (qRT-PCR) and normalized to the level of 18S. *$P < 0.05$ vs. low glucose (LG) 16 h group. Mono-methylation is the predominant H3K4 mark after transient hyperglycemia. Bovine aortic endothelial cells were exposed to glucose and soluble chromatin was immunopurified at the indicated times using H3K4m1 (*B*), H3K4m2 (*C*), and H3K4m3 (*D*) antibodies. qPCR was used to measure the level of enrichment on the NFκB-p65 promoter (-400 bp from the $+1$ transcription start site). Error bars represent SE. Samples were analyzed in triplicate, and data are presented as means ± SE. *$P < 0.05$ vs. LG 16 h group, **$P < 0.01$ vs. LG 16 h group. *E*: Set7 associated histone methyltransferase activity of human FLAG tagged Set7 (Flag-Set7) overexpressed in human endothelial cells and immunoprecipitated using anti-flag antibody. The substrate used to determine methyltransferase activity was recombinant histone H3. *F*: Lysine 4 of histone H3 (H3K4) is a major methylation site for the Set7 enzyme. Set7 was immunoprecipitated by anti-FLAG antibody in overexpressed Set7 or control pCX4neo human endothelial cells. Substrates used to determine methyltransferase activity were synthesized histone H3K4 and mutant H3R4 peptides. *G*: Aortic endothelial cells were exposed to glucose and soluble chromatin were immunopurified at the indicated times with Set7 antibody, and qPCR was used to measure the level of enrichment on the NFκB-p65 promoter. *$P < 0.01$ vs. LG 16 h group. *H*: The osmolyte mannitol does not increase NFκB-p65 mRNA levels. Samples were analyzed in triplicate, and data are presented as means ± SE. *I*: Mannitol does not increase Set7 association with the NFκB-p65 promoter. Samples were analyzed in triplicate, and data are presented as means ± SE.

RESULTS

Previous hyperglycemia is associated with persistent gene activity and H3K4m1. We recently demonstrated that transient hyperglycemia causes gene-activating H3K4m1 marks associated with NFκB-p65 gene expression (3). Despite these and other recent advances, understanding the complexity of H3K4 and H3K9 methylation remains an important challenge. We show that transient hyperglycemia induces long-lasting activation of the NFκB-p65 gene (Fig. 1*A*) and persistent changes in H3K4m1 (Fig. 1*B*), which were not seen for H3K4m2 (Fig. 1*C*) and H3K4m3 (Fig. 1*D*). The epigenetic changes persist for 6 days of subsequent normal glycemia. To differentiate the role of glucose in endothelial cells, we also measured the effect of transient hyperglycemia on the counteracting cytokine, interleukin (IL)-10. Expression of the IL-10 gene

in bovine and human endothelial cells did not change after transient exposure to hyperglycemia (data not shown).
Set7 mono-methylates H3K4 in human vascular cells. Based on this specific change in H3K4m1, but not di-methylation or tri-methylation, we postulated that the Set7 enzyme, previously reported to act as a histone mono-methyltransferase, albeit in nonendothelial cells, might be involved (13). Indeed, because the crystal structure of Set7 (13) indicates specificity for this enzyme as a mono-methylase to its target K4 lysine of histone H3, we tested purified Set7 expressed from human vascular cells. These results show for the first time that expressed Set7 possesses histone methyltransferase activity, as assayed by its ability to methylate histone H3 (Fig. 1*E*). To determine whether H3K4 is the unique methylation site of Set7 activity (14), histone methyltransferase activity of purified
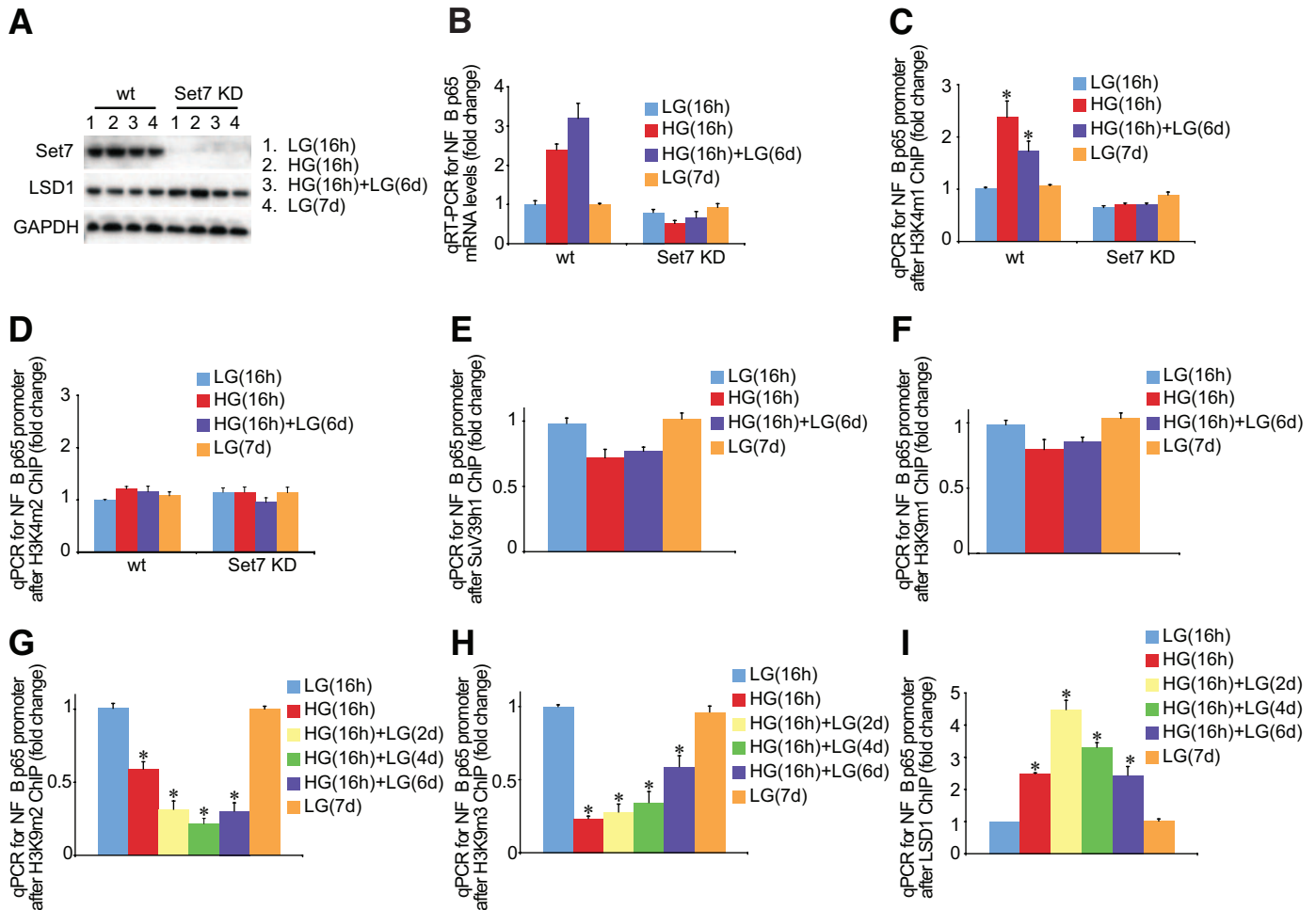
FIG. 2. Erasure of the activating H3K4m1 mark on the NFκB-p65 promoter in Set7 KD cells despite transient hyperglycemia. *A*: Protein blot of Set7 knockdown in HMECs exposed to ambient and prior hyperglycemia for the indicated times. *B*: Ambient and prior hyperglycemia does not sustain increased NFkB-p65 gene expression in Set7 KD cells. RNA was extracted, and NFκB-p65 mRNA levels were quantified by real-time RT-PCR (qRT-PCR) and normalized to the level of 18S. *C*: Knockdown of the Set7 enzyme rescinds H3K4m1 mark on the NFκB-p65 promoter. Samples were analyzed in triplicate, and data are presented as means ± SE. *$P < 0.05$ vs. LG 16 h group. *D*: Set7 KD does not change the H3K4m2 mark on the NFκB-p65 promoter. HMECs were exposed to glucose, and soluble chromatin was immunopurified at the indicated times for SuV39h1 (*E*), H3K9m1 (*F*), H3K9m2 (*G*), H3K9m3 (*H*), and LSD1 (*I*) antibodies. qPCR was used to measure the level of enrichment on the NFκB-p65 promoter. Error bars represent SE. Samples were analyzed in triplicate, and data are presented as means ± SE. *$P < 0.05$ vs. LG 16 h group.

Set7 was assayed using H3K4 and H3R4 as substrate peptides (Fig. 1*F*). The results of these experiments indicate that Set7 has specific H3K4 methylation activity and mutation of the lysine residue to arginine (H3R4) eliminates the ability of the peptide to serve as a substrate for the Set7 histone methyltransferase.

Glucose-induced changes in H3K4m1 are related to the recruitment of Set7. Because Set7 appears to be the enzyme responsible for H3K4m1 in immortalized cancer cell types (14) and is now confirmed in endothelial cells (Fig. 1*E* and *F*), we subsequently tested the hypothesis that Set7 is mobilized to the NFκB-p65 promoter to maintain the active transcriptional state. Immunopurified chromatin from bovine aortic endothelial cells exposed to transient hyperglycemic conditions was associated with sustained enrichment for Set7 on the NFκB-p65 promoter ($P < 0.05$) in response to glucose (Fig. 1*G*). To exclude the possibility that the effects are a result of osmotic stress, cells were incubated in 30 mmol/l mannitol for 16 h and returned to normoglycemia for 2, 4, or 6 days. Analysis of NFκB-p65 gene expression showed no increase in the p65 transcript in response to mannitol stimulation (Fig. 1*H*). Chromatin immunoprecipitation analyses indicated no en-

richment of the Set7 enzyme on the NFκB-p65 promoter consistent with persisting epigenetic marks being mediated by glucose (Fig. 1*I*).

Set7 knockdown attenuates glucose-induced p65 gene activity. Having established that Set7 has methyltransferase activity for H3K4 and specific recruitment to the NFκB-p65 gene, we next determined the functional consequence of knockdown of Set7 on epigenetic persistence of H3K4m1 marks and NFκB-p65 gene expression mediated by transient hyperglycemia. A protein blot of Set7 in wild-type and knockdown (Set7KD) cells indicated robust silencing by the shRNA to Set7 in endothelial cells (Fig. 2*A*). Transient hyperglycemia failed to induce NFκB-p65 gene expression in Set7KD cells (Fig. 2*B*), suggesting that this specific histone methyltransferase is required for glucose-mediated gene activity. We also confirmed that the erasure of NFκB-p65 gene expression depends on changes in histone methylation mediated by Set7 (Fig. 2*C*). Parallel experiments using H3K4m2 antibody were also performed to illustrate the specificity of histone modification with no effect on H3K4m2 seen with Set7KD (Fig. 2*D*). We also assessed IL-10 gene expression in Set7KD and wild-type

cells. The knockdown of Set7 did not change IL-10 mRNA levels in these cells (data not shown).

SuV39h1 has a conserved Set [*S*u(var)3–9, *E*nhancer-of-zeste, *T*rithorax] catalytic domain that belongs to the histone methyltransferase family and is capable of methylating lysine K9 of histone H3 (H3K9) to mediate transcriptional repression. We first determined whether SuV39h1 was inversely correlated with NFκB-p65 transcription and a component of hyperglycemic memory. Soluble chromatin fractions derived from cross-linked HMECs were immunoprecipitated against SuV39h1 antibody and enrichment was compared with baseline glucose controls by real-time PCR quantitation. Chromatin immunopurification analysis indicates that the co-repressor SuV39h1 does not significantly change on the p65 promoter (Fig. 2*E*).

Transient hyperglycemia causes a sustained reduction of H3K9 methylation on the NFκB-p65 promoter. The degree of gene activation or inhibition is exquisitely regulated by multiple histone marks mediated by histone methyltransferase enzymes (15). Indeed, methylation of H3K4 and H3K9 can both inhibit each other and can be mutually antagonistic (14). Therefore, to further elucidate the underlying regulatory mechanism of NFκB-p65 gene expression as a result of transient and prior hyperglycemia in endothelial cells, we specifically investigated these repressive H3K9 methylation marks. Endothelial cells were incubated in high glucose for 16 h and then returned to normoglycemic conditions for 2, 4, or 6 days and analyzed for H3K9m1 (Fig. 2*F*). Chromatin immunoprecipitation measurements indicate that transient hyperglycemia causes a sustained reduction in both H3K9m2 (Fig. 2*G*) and H3K9m3 (Fig. 2*H*) on the NFκB-p65 promoter.

Transient hyperglycemia induces recruitment of LSD1 H3 demethylase. Although we have initially focused on various changes in histone methylation, it is increasingly appreciated that methyl groups can be removed or erased as a result of demethylation (16). Indeed, until recently, it was believed that methyl groups could not be removed and erased from histones. Recent experimental studies now show that demethylation is linked to both transcriptional repression and activation events (17,18). Lysine-specific demethylase 1 (LSD1) and Jumonji C (JmjC) have recently been characterized as H3 demethylases (19–22). LSD1 is a nuclear amine oxidase that uses oxygen as an electron acceptor to reduce methylated lysine to form lysine (20). LSD1 demethylates H3K4m1 and H3K4m2 and is consistent with its role in removal of the active methylation mark; LSD1 is found in co-repressor complexes and promotes suppression of gene expression (16). LSD1 is also associated with the activation of gene expression and demethylation of H3K9m1 and H3K9m2 (19,21,23). The JmjC protein family specifically demethylates H3K9 and is associated with the activation of gene expression (24,25). The preference for distinct H3K9 methylation erasure in the experiments we have performed (Fig. 2*E* and *F*) prompted us to test the hypothesis that demethylation at histone H3 lysine 9 might be associated with the cooperative recruitment of LSD1 at the NFκB p65 gene. The role of the LSD1 enzyme in response to transient hyperglycemia is not well understood, and this is underscored by recent evidence suggesting the release of the demethylase on active genes is inversely linked with increased H3K4m2 (26). With these results in mind and our experimental evidence indicating that transient hyperglycemia could be associated with increased gene-activating

H3K4m1 with no significant change in H3K4m2 or H3K4m3, we examined recruitment of LSD1 demethylase to the p65 promoter in response to hyperglycemia. Results shown in Fig. 2*I* indicate that transient hyperglycemia enriches the demethylase, LSD1, on the NFκB-p65 promoter and that this is inversely correlated with H3K9 methylation, which is consistent with its role as a co-activator of gene activity.

In vivo studies

Metabolic parameters. To explore the in vivo relevance of these changes in p65 expression, we examined changes in expression of NFκB-p65 not only in a well-validated model of diabetes-associated atherosclerosis, the diabetic apoE KO mice (27), but also have evaluated these changes in a group of mice where there has been a degree of β-cell recovery weeks after induction of diabetes, as has been previously reported with respect to streptozocin in rodents (28). This subgroup of mice has experienced a period of hyperglycemia followed by a significant period of near-normoglycemia (HG→NG), allowing us to determine if previous transient episodes of hyperglycemia can lead to sustained upregulation of genes implicated in diabetic vascular injury.

Glycated hemoglobin was increased significantly in the diabetic apoE KO group ($17.6 \pm 0.4\%$, $n = 15$) when compared with the control apoE KO group ($4.7 \pm 0.1\%$, $n = 15$). Both these parameters were decreased in the previously hyperglycemic group but were still elevated ($6.4 \pm 0.8\%$, $n = 10$), albeit modestly, when compared with the control apoE KO group ($P < 0.05$). Body weight was significantly decreased in the diabetic apoE KO group (20.9 ± 0.4 g) compared with control apoE KO mice (30.7 ± 0.3 g, $P < 0.01$). Mice in the previously hyperglycemic group had a modest decrease in body weight (27.0 ± 1.0 g) when compared with control apoE KO mice ($P < 0.05$) but not as low as seen in diabetic apoE KO mice ($P < 0.01$). Plasma lipids including total and LDL cholesterol were increased in diabetic apoE KO mice but were similar to control mice in the previously hyperglycemic animals (total cholesterol, control 14.5 ± 0.7 mmol/l [means $\pm$ SE], diabetic 33.0 ± 4.6 mmol/l [$P < 0.01$ vs. control], previously hyperglycemic 15.5 ± 1.3 mmol/l [$P < 0.01$ vs. diabetic]; LDL cholesterol, control 10.4 ± 0.6 mmol/l, diabetic 27.2 ± 4.4 mmol/l [$P < 0.01$ vs. control], previously hyperglycemic 10.5 ± 2.8 mmol/l [$P < 0.01$ vs. diabetic]).

Plaque area remained increased and NFκB, VCAM, and MCP-1 mRNA levels remained elevated in previously hyperglycemic mice. Plaque area was quantitated as a percentage area of aorta stained red with Sudan IV. Total plaque area was significantly increased in diabetic apoE mice (HG→HG) and was compared with control apoE mice (NG→NG) (Table 1). Importantly, the greater-than-threefold increase in plaque area was also seen in the previously hyperglycemic (HG→NG) mice. When plaque area was quantified in the three individual segments (arch, thoracic, and abdominal region), the same pattern was observed as for total plaque area with an increase in plaque area at all three sites in diabetic mice and a similar increase at these sites in the previously hyperglycemic mice (Fig. 3). Aortic mRNA levels for NFκB p65 were significantly upregulated in diabetic apoE KO mice when compared with the apoE KO controls (Table 2). NFκB p65 gene expression was also significantly upregulated in the aortas from the previously hyperglycemic mice. Gene expression of two important mediators of atherosclerosis,

TABLE 1
Total and arch plaque area was quantitated as a percentage area of aorta stained red with Sudan IV in control apoE KO, diabetic apoE KO, and previously hyperglycemic apoE KO mice

	n	Total	Arch	Thoracic	Abdominal
Control apoE KO (NG→NG)	10	3.0 ± 0.5	8.0 ± 0.5	1.2 ± 0.3	1.1 ± 0.3
Diabetic apoE KO (HG→HG)	10	13.0 ± 1.0*	24.4 ± 1.0*	8.7 ± 1.0*	8.5 ± 0.7*
Previously hyperglycemic apoE KO (HG→NG)	6	11.4 ± 1.9*	21.3 ± 2.1*	8.0 ± 2.7*	8.2 ± 1.8*

Data are means ± SE. *$P < 0.05$ compared with the control apoE KO group.

particularly in the diabetic setting, that are known to be NFκB dependent—VCAM-1 (11) and MCP-1 (29)—were also significantly upregulated in the chronically diabetic mice. This increase in MCP-1 and VCAM-1 mRNA levels was also observed in the aortas from the previously hyperglycemic mice (Table 2).

DISCUSSION

The novel findings described in these in vitro studies represent a paradigm shift in understanding the relationship between epigenetic change and hyperglycemic memory. Using endothelial cell models of transient and prior hyperglycemia, we demonstrated that active NFκB-p65 gene expression is linked to persisting epigenetic marks that are maintained when the cell is removed from its hyperglycemic environment. The evidence for this came from cell culture experiments in which specified changes in epigenetic information are associated with transcriptional longevity. Three sets of experiments indicated that the underlying regulatory mechanism of NFκB-p65 gene activity induced by hyperglycemia involve specific epigenetic modifications. First, the persistence of NFκB-p65 gene activation mediated by transient hyperglycemia is associated with Set7 recruitment and H3K4 mono-methylation, which could be overcome by somatic knockdown of the Set7 methyl-lysine writer. Second, the consequent increase in activating epigenetic marks is directly correlated with distinct and persistent H3K9 demethylation events. Finally, chromatin immunopurification studies indicate hyperglycemia-induced recruitment of the methyl-lysine eraser, LSD1, occurs concomitantly with reduced H3K9 methylation and increased NFκB-p65 expression. Although none of the experiments alone constitutes evidence that any one epigenetic mark is solely important in long-lived gene activity, taken together, the evidence strongly suggests that changes in epigenetic information are associated and potentially could partly explain the phenomenon of "hyperglycemic memory."

The importance of sustained effects of previous changes in glucose levels is increasingly being appreciated as a result of more recent findings from studies of vascular
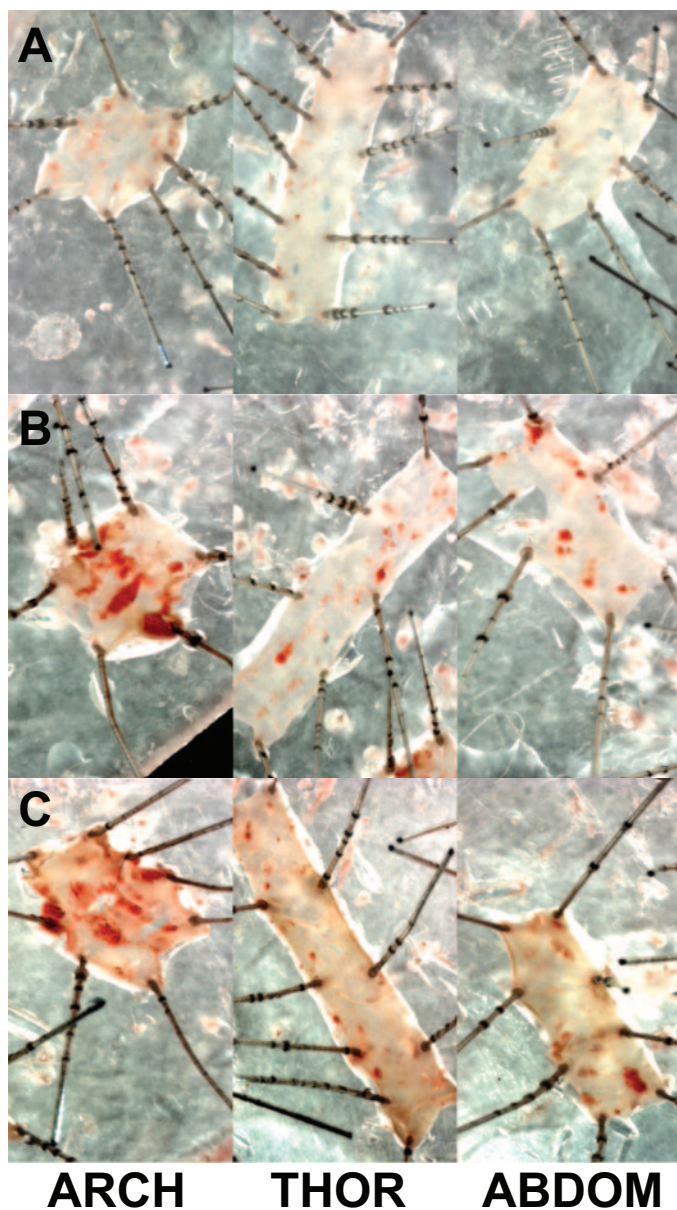

FIG. 3. Plaque area remained increased in the previously hyperglycemic mice. Atherosclerotic plaques in aorta staining in red with picro sirus red solution in control apoE KO (*A*), diabetic apoE KO (*B*), and previously hyperglycemic apoE KO mice (*C*). ABDOM, abdominal; THOR, thoracic. (A high-quality digital representation of this figure is available in the online issue.)

TABLE 2
mRNA expression of NFκB-p65, MCP-1, and VCAM in control apoE KO, diabetic apoE KO, and previously hyperglycemic apoE KO mice

	n	NFκB-p65	MCP-1	VCAM-1
Control apoE KO (NG→NG)	5	1.0 ± 0.2	1.1 ± 0.2	1.0 ± 0.2
Diabetic apoE KO (HG→HG)	5	2.5 ± 0.9*	3.2 ± 1.1*	3.2 ± 0.5*
Previously hyperglycemic apoE KO (HG→NG)	4	2.7 ± 1.1*	3.7 ± 0.9*	1.9 ± 0.06*†

Data are means ± SE. *$P < 0.05$ compared with control apoE KO group; †$P < 0.05$ compared with diabetic apoE KO group.

disease in type 1 and type 2 diabetes. For example, the identification of a long-term impact on cardiovascular events as a result of previous periods of altered glycemic control in the DCCT has emphasized this phenomenon of "metabolic memory" (2). More recently, the long-term outcomes, in particular cardiovascular outcomes, from the UKPDS suggest that the period of intensive glycemic control that occurred more than a decade ago and initially did not demonstrate statistically significant reductions in macrovascular disease, now shows clear benefits on a range of cardiovascular end points including mortality (30). It remains to be determined as to the underlying explanation for these persistent, ongoing injurious effects to diabetic vessels as a result of previous hyperglycemia. However, the recent demonstration by several groups of various epigenetic changes as a result of hyperglycemia (3,26) and, in particular in this study, certain changes in enzymes involved in histone methylation and demethylation emphasizes the potential long-term effects of glucose on processes linked to gene expression. This study focused on histone methylation changes in response to transient hyperglycemia, illustrating that distinct H3K4 and H3K9 methylation patterns on the NFκB-p65 gene coexist to regulate gene expression, and these methyl-marks are probably associated with the activity of methyl-writing and -erasing enzymes on the promoter. Interestingly, other evidence suggests that H3K4m2 is increased on genes activated by hyperglycemia, which was recently postulated to be inversely correlated with LSD1 (26). Although these distinguishable results indicate a complicated and somewhat contradictory set of experimental data, we cannot exclude that these distinct differences indicate functional specialization of H3 enzymes in the various vascular cell populations.

To further explore the potential in vivo relevance of the changes associated with p65 gene expression, we used an extensively characterized model of diabetes-associated atherosclerosis (11,27). In this model, a subgroup of diabetic animals lost their severe hyperglycemia, as has previously been reported after injection of streptozotocin in various rodent models of diabetes (28,31,32). Despite a reduction in plasma glucose and lipid levels at death in these previously hyperglycemic mice, p65 gene upregulation persisted, as did the increase in gene expression of various NFκB-dependent proteins, MCP-1, and VCAM-1. Furthermore, the sustained increase in these pro-inflammatory molecules was associated with increased atherosclerosis in these mice with prior hyperglycemia. These changes are consistent with this model, exhibiting macrovascular disease as a result of "metabolic memory."

Thus, it appears that periods of transient or prior hyperglycemia lead to various methylation and demethylation events that, when integrated, have an impact on gene activity. These events lead to sustained activation of pro-inflammatory pathways, which are likely to participate in the progression of diabetic complications. Further understanding of the chromatin remodeling events and how they are linked to ongoing vascular changes in diabetes should lead to better strategies to reduce the burden of diabetes complications.

REFERENCES

1. Epidemiology of Diabetes Interventions and Complications (EDIC) Study Group. Sustained effect of intensive treatment of type 1 diabetes mellitus on development and progression of diabetic nephropathy. JAMA 2003;290:2159–2167
2. Nathan DM, Cleary PA, Backlund JY, Genuth SM, Lachin JM, Orchard TJ, Raskin P, Zinman B. Intensive diabetes treatment and cardiovascular disease in patients with type 1 diabetes. N Engl J Med 2005;353:2643–2653
3. El-Osta A, Brasacchio D, Yao D, Pocai A, Jones PL, Roeder RG, Cooper ME, Brownlee M. Transient high glucose causes persistent epigenetic changes and altered gene expression during subsequent normoglycemia. J Exp Med 2008;205:2409–2417
4. Chalmers J, Cooper ME. UKPDS and the legacy effect. N Engl J Med 2008;359:1618–1620
5. Patel A, MacMahon S, Chalmers J, Neal B, Billot L, Woodward M, Marre M, Cooper M, Glasziou P, Grobbee D, Hamet P, Harrap S, Heller S, Liu L, Mancia G, Mogensen CE, Pan C, Poulter N, Rodgers A, Williams B, Bompoint S, de Galan BE, Joshi R, Travert F. Intensive blood glucose control and vascular outcomes in patients with type 2 diabetes. N Engl J Med 2008;358:2560–2572
6. Gerstein HC, Miller ME, Byington RP, Goff DC Jr, Bigger JT, Buse JB, Cushman WC, Genuth S, Ismail-Beigi F, Grimm RH Jr, Probstfield JL, Simons-Morton DG, Friedewald WT. Effects of intensive glucose lowering in type 2 diabetes. N Engl J Med 2008;358:2545–2559
7. Roy S, Sala R, Cagliero E, Lorenzi M. Overexpression of fibronectin induced by diabetes or high glucose: phenomenon with a memory. Proc Natl Acad Sci U S A 1990;87:404–408
8. Mack CP. An epigenetic clue to diabetic vascular disease. Circ Res 2008;103:568–570
9. Okabe J, Eguchi A, Wadhwa R, Rakwal R, Tsukinoki R, Hayakawa T, Nakanishi M. Limited capacity of the nuclear matrix to bind telomere repeat binding factor TRF1 may restrict the proliferation of mortal human fibroblasts. Hum Mol Genet 2004;13:285–293
10. Akagi T, Sasai K, Hanafusa H. Refractory nature of normal human diploid fibroblasts with respect to oncogene-mediated transformation. Proc Natl Acad Sci U S A 2003;100:13567–13572
11. Candido R, Jandeleit-Dahm KA, Cao Z, Nesteroff SP, Burns WC, Twigg SM, Dilley RJ, Cooper ME, Allen TJ. Prevention of accelerated atherosclerosis by angiotensin-converting enzyme inhibition in diabetic apolipoprotein E-deficient mice. Circulation 2002;106:246–253
12. Thomas MC, Tikellis C, Burns WM, Bialkowski K, Cao Z, Coughlan MT, Jandeleit-Dahm K, Cooper ME, Forbes JM. Interactions between renin angiotensin system and advanced glycation in the kidney. J Am Soc Nephrol 2005;16:2976–2984
13. Xiao B, Jing C, Wilson JR, Walker PA, Vasisht N, Kelly G, Howell S, Taylor IA, Blackburn GM, Gamblin SJ. Structure and catalytic mechanism of the human histone methyltransferase SET7/9. Nature 2003;421:652–656
14. Wang H, Cao R, Xia L, Erdjument-Bromage H, Borchers C, Tempst P, Zhang Y. Purification and functional characterization of a histone H3-lysine 4-specific methyltransferase. Mol Cell 2001;8:1207–1217
15. Ruthenburg AJ, Allis CD, Wysocka J. Methylation of lysine 4 on histone H3: intricacy of writing and reading a single epigenetic mark. Mol Cell 2007;25:15–30
16. Shi Y, Sawada J, Sui G, Affar el B, Whetstine JR, Lan F, Ogawa H, Luke MP, Nakatani Y, Shi Y. Coordinated histone modifications mediated by a CtBP co-repressor complex. Nature 2003;422:735–738
17. Metzger E, Schule R. The expanding world of histone lysine demethylases. Nat Struct Mol Biol 2007;14:252–254

18. Trojer P, Reinberg D. Histone lysine demethylases and their impact on epigenetics. Cell 2006;125:213–217
19. Metzger E, Wissmann M, Yin N, Muller JM, Schneider R, Peters AH, Gunther T, Buettner R, Schule R. LSD1 demethylates repressive histone marks to promote androgen-receptor-dependent transcription. Nature 2005;437:436–439
20. Shi Y, Lan F, Matson C, Mulligan P, Whetstine JR, Cole PA, Casero RA, Shi Y. Histone demethylation mediated by the nuclear amine oxidase homolog LSD1. Cell 2004;119:941–953
21. Wissmann M, Yin N, Muller JM, Greschik H, Fodor BD, Jenuwein T, Vogler C, Schneider R, Gunther T, Buettner R, Metzger E, Schule R. Cooperative demethylation by JMJD2C and LSD1 promotes androgen receptor-dependent gene expression. Nat Cell Biol 2007;9:347–353
22. Tsukada Y, Fang J, Erdjument-Bromage H, Warren ME, Borchers CH, Tempst P, Zhang Y. Histone demethylation by a family of JmjC domain-containing proteins. Nature 2006;439:811–816
23. Lan F, Zaratiegui M, Villen J, Vaughn MW, Verdel A, Huarte M, Shi Y, Gygi SP, Moazed D, Martienssen RA. S. pombe LSD1 homologs regulate heterochromatin propagation and euchromatic gene transcription. Mol Cell 2007;26:89–101
24. Klose RJ, Yamane K, Bae Y, Zhang D, Erdjument-Bromage H, Tempst P, Wong J, Zhang Y. The transcriptional repressor JHDM3A demethylates trimethyl histone H3 lysine 9 and lysine 36. Nature 2006;442:312–316
25. Yamane K, Toumazou C, Tsukada Y, Erdjument-Bromage H, Tempst P, Wong J, Zhang Y. JHDM2A, a JmjC-containing H3K9 demethylase, facilitates transcription activation by androgen receptor. Cell 2006;125:483–495
26. Reddy MA, Villeneuve LM, Wang M, Lanting L, Natarajan R. Role of the lysine-specific demethylase 1 in the proinflammatory phenotype of vascular smooth muscle cells of diabetic mice. Circ Res 2008;103:615–623
27. Hsueh W, Abel ED, Breslow JL, Maeda N, Davis RC, Fisher EA, Dansky H, McClain DA, McIndoe R, Wassef MK, Rabadan-Diehl C, Goldberg IJ. Recipes for creating animal models of diabetic cardiovascular disease. Circ Res 2007;100:1415–1427
28. Kennedy JM, Zochodne DW. Experimental diabetic neuropathy with spontaneous recovery: is there irreparable damage? Diabetes 2005;54:830–837
29. Candido R, Allen TJ, Lassila M, Cao Z, Thallas V, Cooper ME, Jandeleit-Dahm KA. Irbesartan but not amlodipine suppresses diabetes-associated atherosclerosis. Circulation 2004;109:1536–1542
30. Holman RR, Paul SK, Bethel MA, Matthews DR, Neil HA. 10-year follow-up of intensive glucose control in type 2 diabetes. N Engl J Med 2008;359:1577–1589
31. Hartmann K, Besch W, Zuhlke H. Spontaneous recovery of streptozotocin diabetes in mice. Exp Clin Endocrinol 1989;93:225–230
32. Lake SP, Chamberlain J, Husken P, Bell PR, James RF. In vivo assessment of isolated pancreatic islet viability using the streptozotocin-induced diabetic nude rat. Diabetologia 1988;31:390–394

University Library

MINERVA ACCESS

A gateway to Melbourne's research publications

Author/s:
Brasacchio, D;Okabe, J;Tikellis, C;Balcerczyk, A;George, P;Baker, EK;Calkin, AC;Brownlee, M;Cooper, ME;El-Osta, A

Title:
Hyperglycemia Induces a Dynamic Cooperativity of Histone Methylase and Demethylase Enzymes Associated With Gene-Activating Epigenetic Marks That Coexist on the Lysine Tail

Date:
2009-05-01

Citation:
Brasacchio, D., Okabe, J., Tikellis, C., Balcerczyk, A., George, P., Baker, E. K., Calkin, A. C., Brownlee, M., Cooper, M. E. & El-Osta, A. (2009). Hyperglycemia Induces a Dynamic Cooperativity of Histone Methylase and Demethylase Enzymes Associated With Gene-Activating Epigenetic Marks That Coexist on the Lysine Tail. DIABETES, 58 (5), pp.1229-1236. https://doi.org/10.2337/db08-1666.

Persistent Link:
http://hdl.handle.net/11343/264645

License:
CC BY-NC-ND